J. Fluid Mech. (1979), *vol.* 94, *part* 3, *pp.* 477–495
Printed in Great Britain

The dynamics of the head of a gravity current advancing over a horizontal surface

By J. E. SIMPSON AND R. E. BRITTER†
Department of Applied Mathematics and Theoretical Physics, University of Cambridge

(Received 19 April 1978 and in revised form 6 March 1979)

The motion behind the head of a gravity current advancing over a no-slip horizontal surface is a complex three-dimensional flow. There is intense mixing between the current and its surroundings and the foremost part of the head is raised above the surface. Experimental results are obtained from (i) an apparatus in which the head is brought to rest by using an opposing flow and a moving floor and (ii) a modified lock exchange flow. The dimensionless velocity of advance, rate of mixing between the two fluids and the depth of the mixed layer left behind the head and above the following gravity current are determined for an extended range of the dimensionless gravity current depth. The mixing between the two fluids is the result of gravitational and shear instabilities at the gravity current head. A semi-empirical analysis is presented to describe the results. The influence of Reynolds number is discussed and comparison with a documented atmospheric flow is presented.

1. Introduction

Gravity-driven currents (density currents or buoyancy currents) occur in many natural and man-made situations. They occur in the ocean where the flow is driven by salinity and/or temperature inhomogeneities or as turbidity currents on the ocean floor, the density difference being supplied by suspended particles (Allen 1971). In the atmosphere, sea-breeze fronts (Simpson, Mansfield & Milford 1977) and thunderstorm outflows (Lawson 1971 and Hall, Neff & Frazier 1976) are gravity currents of cool air while powder-snow avalanches consist of snow-laden air. Oil spillage on the sea surface (Hoult 1972), spreading of hot water discharged from power stations and the accidental release of dense industrial gases are a few of many industrial problems in which gravity-driven flows are important. In the study of such flows, whether restricted to a parallel-sided channel or not, understanding the dynamics of the head of the gravity current is important, and it may set a necessary boundary condition on the flow which follows it.

The shadowgraph in figure 1 (plate 1) displays some of the essential features of the head of a gravity current advancing along a horizontal surface. The current, about 1% denser than its surroundings, is visible beneath the dark horizontal line. It has nearly constant depth, h_4, of 1 cm and the total depth, h_1, of the two fluids is 15 cm. The head is travelling to the right with a velocity U_1 and the foremost point, indicated by an arrow, is slightly elevated above the surface. There is intense mixing between

† Also Department of Geosciences, North Carolina State University.

0022-1120/79/4321-7450 $02.00

the two fluids near the leading edge of the gravity current, the mixed fluid being left behind the head above the following gravity current. The depth of this layer, h_3, is about 3 cm.

In this paper we investigate the dependence of the velocity of advance of the gravity current head, U_1, on the densities ρ_2 and ρ_1 of the two fluids, the length scales h_4 and h_1 and the acceleration due to gravity, g. Since $\rho_2 \simeq \rho_1$ in the class of flows we are considering, we can introduce the Boussinesq approximation to reduce the variables (ρ_1, ρ_2, g) to $g' = (\rho_2 - \rho_1) g/\rho_1$.

We quantify the observed mixing between the two fluids, that is, the volume flux per unit width, Q, of dense fluid mixed *out* of the gravity current head and we also measure the vertical extent, h_3, of the mixed fluid above the following flow. We seek, as functions of the fractional depth h_4/h_1, three dimensionless variables which together characterize much of the dynamics and structure of the gravity current head, $U_1/(g'h_4)^{\frac{1}{2}}$, Qg'/U_1^3 and h_3/h_4. No dependence on Reynolds number is introduced as we believe that the influence of viscous forces is not important at the Reynolds numbers of interest. (This point is pursued further in § 5.)

Several previous experimental studies of gravity current heads have used a lock-exchange flow (O'Brien & Cherno 1934; Keulegan 1957; Yih 1965; Barr 1967) in which a vertical gate separating salt and fresh water is opened suddenly and the salt water flows under the over-riding fresh water. The flow is symmetrical when the density difference is small and both upper and lower surfaces are rigid. Breaking waves occur on the interface at the heads of the gravity currents and as the flow develops the head no longer fills half the depth. In such lock-exchange experiments the velocity of the head rises from zero after removal of the gate and quickly attains a near-constant value; however, when accurate measurements of the head are attempted it becomes clear that the head is not in a steady state. During an experiment the velocity of advance of the head, the depth of the flow behind the head, the height of the head and the density difference between the head and its surroundings may all slowly vary. Although the lock-exchange flow reduces the independent variable h_4/h_1 to a dependent variable of limited range, measurement of the rate of advance of the head and corresponding length scales are easily made up using a lock exchange and in § 2 we describe a modified procedure in which h_4/h_1 may be varied over an extended range.

To avoid some of the restrictions imposed by the lock exchange flow, an experimental flume with a moving floor was used to investigate the behaviour of the heads of gravity currents of saline solution moving horizontally through water. The heads were brought to rest by varying the value of the opposing flow and the equal floor speed. This arrangement is equivalent to the gravity current head in a lock exchange flow viewed in co-ordinates moving with the head. Examination of gravity current heads in a steady state makes it possible to measure with greater confidence the effects of a variation in both the depth of the flow behind the head and the total depth of the two fluids on the rate of advance and on the structure of the head.

The experimental technique of holding the gravity current head stationary in laboratory co-ordinates was exploited by Britter & Simpson (1978). In that paper (henceforth referred to as BS) experiments were described in which the influence of the no-slip condition under the head was made negligible. The foremost point of the head remained on the floor, and the shape of the head was generally similar to that predicted by von Kármán (1940) and Benjamin (1968) except that intense

mixing was observed between the two fluids at the head; the mixing fluid being left behind the gravity current head. The mixing between the two fluids, previously ignored in analyses of the gravity current head, was included in an analysis in which solutions were obtained for the Froude number, $U_1/(g'h_4)^{\frac{1}{2}}$, and h_3/h_1, and a non-dimensional rate of mixing at the head. It was found that the mixing mechanism was quantitatively similar to Kelvin–Helmholtz instability. Appeal to existing experimental data on this instability led to solutions obtained without the need for independent specification of the rate of mixing between the fluids. Good agreement was obtained between analysis and experiment which, it is thought, are representative of gravity currents running under a clean, free surface in the absence of significant surface tension forces.

Gravity current heads advancing over a horizontal surface are subject to a no-slip condition at the surface, which results in a complicated three-dimensional structure of shifting lobes and clefts. Details of the evolution of this structure have been described by Simpson (1969, 1972) and interpreted as a consequence of the gravitational instability of the less dense fluid over-run by the gravity current head.

The light fluid is ingested underneath the gravity current head, rises due to gravitational instability and is carried forward by motions inside the head, mostly in the neighbourhood of the clefts. Studies with dye tracers led us to conclude that the depth of the over-run less dense fluid is very small, about a tenth of the height of the foremost point of the head, and the flux of light fluid flowing under the head is estimated to be of the order of 0·01 of the flux of light fluid involved in mixing at the top of the head. Though the momentum change of this fluid as it passes through the head is insignificant compared with other momentum changes near the head, it is essential for the lobe and cleft formation and it affects the mixing process at the head. When the gravity current head is advancing over a boundary with slip as in BS, the mixing process at the head is due to the shear instability at the interface and subsequent growth to finite amplitude billows. In the present experiments such an instability is still present (figure 1) but is confused and complicated by the lobe and cleft structure resulting from the gravitational instability of the over-run fluid. The shear instability is more easily seen when slit lighting is used, rather than a shadowgraph, and has been photographed by Simpson (1969).

A two-dimensional mean head profile has been measured by Braucher (1950), Keulegan (1958) and others and these all show the foremost part of the head slightly elevated above the surface. Measurements of the Froude number $U_1/(g'h_4)^{\frac{1}{2}}$ for lock exchange experiments are generally smaller than that predicted by the analysis of Benjamin (1968) or of BS, and we shall follow up Benjamin's (1968) comment that this reduction in Froude number is a result of the raising of the stagnation point (defined in a frame of reference moving with the head) above the surface. Introduction of a two-dimensional model of the flow within the head with the stagnation point elevated above the surface enables extension of the analysis used in BS to the head of a gravity current moving along a no-slip surface. In this paper we present an extensive experimental study of gravity current heads with particular attention to three important, but hitherto experimentally overlooked, aspects: the influence of the fractional depth; the mixing between the two fluids at the head; and the elevation of the foremost point of a head. Early analyses ignored all three aspects, while Benjamin (1968) introduced the first and made passing reference to the latter two.

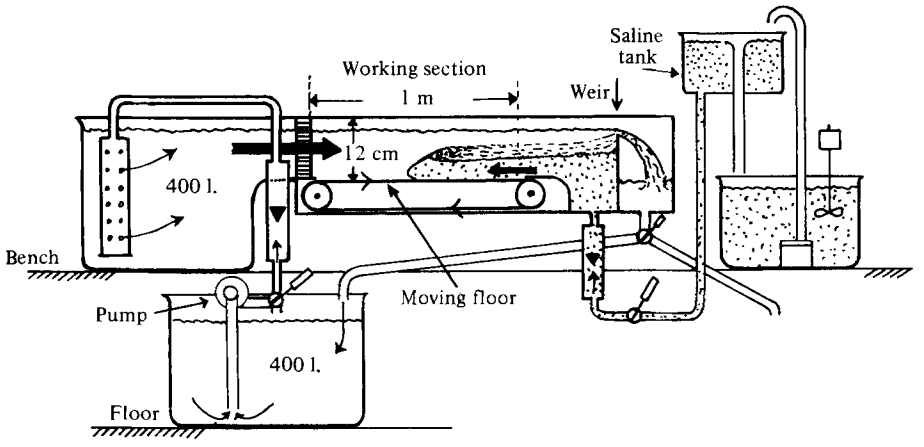

FIGURE 2. Apparatus for maintaining the head of a gravity current in a steady state. A metered flow of water runs from the top reservoir on the left through a flow straightener into the working section. The floor can be moved in the same direction, and the gravity current brought to rest. The input of saline flow corresponding to the rate of mixing at the gravity current head is also metered. The flow over the weir can be either drained or recycled.

2. Experimental apparatus and procedure

The apparatus used for some of the experiments to be described was designed and built in order to study the behaviour of a gravity current head in as near as possible a steady state. The general arrangement of the apparatus is almost identical with that described in BS and is shown in figure 2. A steady current of water is pumped through the working section, the floor of the tank is moved in the same direction in the form of an endless belt and a saline flow is introduced at the downstream end. By suitable selection of U_1, the speed of both the opposing flow and the moving floor, it was possible to bring the head of the saline flow to rest.

At a constant total depth of flow and with a constant input of saline solution in any one experiment, it is easy to arrest the gravity current head and it is normally brought to rest less than half way along the working section. The flow of dense fluid behind the head is maintained against friction by a small slope in the density surface and small changes in opposing flow and floor speed can be counteracted by a forward or backward motion of the head. This leads to a change in h_4, the depth of the dense fluid immediately behind the head.

In each experiment the total depth, h_1, is set up by the weir, and this can vary between 6 and 12 cm. A fixed rate of saline input, Q per unit width of tank, with $(\rho_2-\rho_1)/\rho_1$ between 0·0037 and 0·03 is then established. When the front has been brought to rest by selection of a suitable value of flow and floor speed U_1 (the available range is from 0 to 6 cm s^{-1}), the value of h_4 is recorded, either by marking on a shadowgraph screen or by photography.

In each case we measured the total head height, h_3+h_4, that is, the height from the ground to the top of the billows forming on the head before they began to break up and lose a clear outline. It was found that the depth of the mixing layer behind the head was equal, within the limits of experimental accuracy, to the height of the top of the billow region above the dense layer.

Mean velocity measurements were made using a DISA hot-film probe with a DISA constant temperature anemometer. Care was taken to reduce the error due to temperature sensitivity of the probe. Mean velocity measurements were accurate to within 5 % for velocities greater than 1 cm/s. Mean salinity measurements were made with a conventional conductivity meter based on a design of the Hydraulic Research Station at Wallingford, England. These measurements are accurate to within 5 % also. The profiles of velocity and salinity were made between $10h_4$ and $15h_4$ behind the foremost part of the head. Further details of the monitoring of the flows and of the accuracy to be expected in the results are dealt with in BS and will not be repeated here.

Figure 3 (plate 1) shows a photograph of a typical gravity current head with $(\rho_2-\rho_1)/\rho_1 = 0{\cdot}0074$ brought to rest in a flow of total depth 8 cm. The floor and flow speeds are identical; this flow corresponds to a gravity current moving forward into calm surroundings, and billows resembling Kelvin–Helmholtz billows can be seen forming on the head. The height h_4 is taken as the lowest dark horizontal line as soon as it becomes clearly marked behind the area of the head, and this was found to be consistent with the velocity measurements made with the hot-film probe and the salinity measurements. In practice it was found easier to determine the value of h_4 from the shadowgraphs than it may appear from still photographs, and its value is normally well defined because of the small slope of the boundary of the top of the flow following the head.

A series of measurements was also made in a tank 180 cm long, 10 cm wide and 20 cm high using a modified lock exchange in which gravity currents of low fractional depth h_4/h_1 were generated. In this lock-exchange method the lock was only filled to a fraction $1/n$ of its depth with the denser fluid, and the rest filled with the less dense fluid. In some of the experiments to be described measurements were made with $n = 1$, 1·5, 2, 3, 4 and 5, obtaining velocities of advance and head-heights for values of h_4/h_1 varying between 0·33 and 0·05. The shadowgraphs in figures 1 and 4 show flows near the extremes of the range. Figure 4 (plate 2) shows a lock-exchange flow with $n = 1$ and with a central gate as described by Yih (1965). The front has already advanced a distance of about 28 cm (between 5 and 6 times the depth of the lock) from the former position of the gate at the left of the photograph, but earlier both the main interface and the top of the head were unsteady and indistinct. The value of h_4/h_1 shown here is 0·33, the largest value obtained in our experiments, and it is of interest to note that Benjamin (1968) suggested that flows with h_4/h_1 in the range 0·5–0·347 would be impossible to produce experimentally. Figure 1, already referred to in § 1, shows a lock-exchange flow in which the initiating lock was filled to a quarter of its depth with the denser liquid. The value of h_4/h_1 is 0·06, and the total head height is 4·5 times the depth of the following flow.

3. Experimental results

3.1. *Velocity measurements*

An experimental solution to the question raised in § 1 as to what is the velocity of advance of the gravity current head in terms of the density difference and characteristic length scales is shown in figure 5. The velocity of advance has been made non-dimensional by forming the Froude number $U_1/(g'h_4)^{\frac{1}{2}}$ and is plotted as a function of the fractional depth h_4/h_1. The open symbols are data from the steady-state experiments

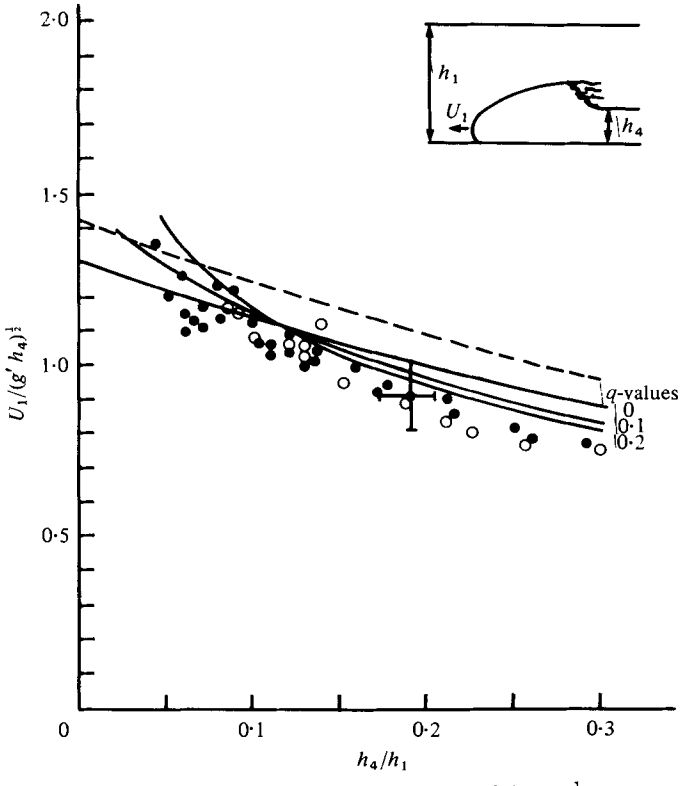

FIGURE 5. Experimental values of the Froude number $U_1/(g'h_4)^{\frac{1}{2}}$, based on the depth of the following steady flow, plotted against h_4/h_1, the fractional depth. ○ data points from steady-state apparatus. ● data from modified lock-exchange experiments. The theoretical curves for the non-dimensional volume flux $q = Qg'/U_1^3 = 0$, 0·1 and 0·2 are also plotted. The dashed line is a theoretical curve from Benjamin (1968) for a flow with no mixing at the gravity current head and with the stagnation point on the ground.

while the closed symbols are from the modified lock-exchange flow, and no systematic differences appear between the data obtained from the two experimental techniques. The Froude number is seen to decrease with increasing fractional depth from about 1·3 at $h_4/h_1 \simeq 0{\cdot}05$ to about 0·75 at $h_4/h_1 \simeq 0{\cdot}3$, and error estimates are included as the two perpendicular bars about one of the data points. The lower limit to the range of h_4/h_1 is set by the difficulty of keeping the Reynolds number large while attempts to form a flow at a larger fractional depth than 0·33 were unsuccessful and this limit has already been commented upon in § 2.

The effects of Reynolds number on the non-dimensional velocity of advance have been considered in some detail by other authors (Keulegan 1957, 1958; Barr 1967), who have proposed limits for Reynolds number independence. Unless stated to the contrary the results presented here are for $5000 > U_1 h_4/\nu > 500$; at smaller Reynolds numbers we observed that the non-dimensional velocity of advance, the rate of mixing between the two fluids and the non-dimensional head height h_3/h_4 all become smaller. An alternative Froude number $U_1/(g'h_1)^{\frac{1}{2}}$ has been used by some authors; however this Froude number is less appropriate at small fractional depths when the total depth of the two fluids becomes less important.

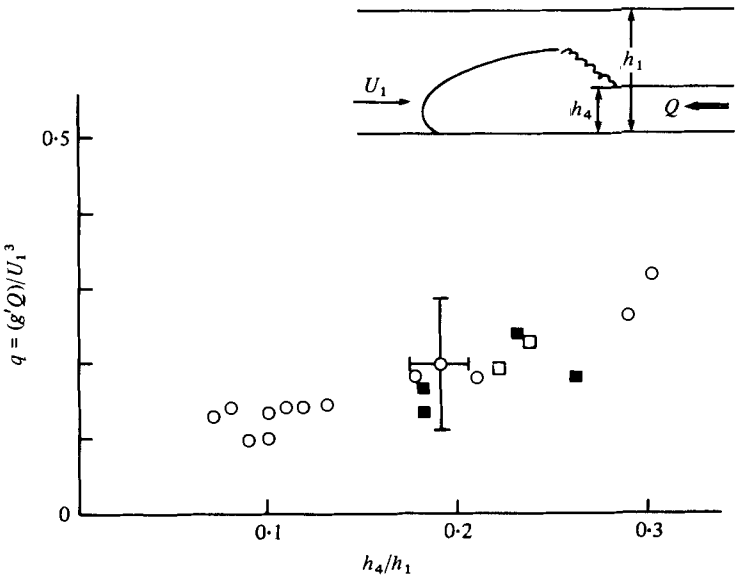

FIGURE 6. Values of non-dimensional volume flux $q = g'Q/U_1^3$ with fractional depth h_4/h_1. ○ from steady-state apparatus, Q and U_1 measured through rotameters. ■ from steady-state apparatus measurements from velocity profiles as described in the text. □ from dye-patches in lock exchange flows.

3.2. *Mixing rate*

The rate of mixing between the two fluids or, more precisely, the rate, Q, at which dense fluid is mixed *out* of the gravity current by the less dense fluid at the gravity current head has been non-dimensionalized with g' and U_1 to form the variable $q = Qg'/U_1^3$ and plotted against the fractional depth in figure 6. The open circles are data taken from the steady-state experiments using the measured values of Q and U_1, the closed squares are from steady-state experiments but obtained by integrating the velocity profile in the lower dense layer. The open squares are taken from lock exchange flows by integrating the velocity profile in the lower dense layer where the velocity profile was determined by timing dye patches. All three techniques are in reasonable agreement but are subject to large errors indicated by the perpendicular bars. The non-dimensional mixing rate increases from about 0·13 at $h_4/h_1 \simeq 0{\cdot}1$ to about 0·25 at $h_4/h_1 \simeq 0{\cdot}3$.

An alternative non-dimensionalizing of the mixing flux Q is with the velocity of advance U_1 and the length scale h_4 to form Q/U_1h_4. But as Q/h_4 is a mean velocity of dense fluid arriving at the gravity current head, an 'overtaking velocity' U_4, the mixing at the gravity current head may be expressed as the velocity ratio U_4/U_1. This ratio was found to be nearly independent of h_4/h_1 with a mean value of $U_4/U_1 = 0{\cdot}16 \pm 0{\cdot}04$. (The $\pm$ refers, here and elsewhere, to $\pm$ one standard deviation from the mean of the experimental results.) Thus the mean velocity in the gravity current immediately behind the gravity current head is approximately $\frac{1}{6}$ greater than the velocity of advance of the head. It should be noted that the no-slip condition at the lower boundary has produced a velocity profile in the gravity current and that the maximum velocity in the gravity current may be significantly greater than the mean velocity $U_1 + U_4$.

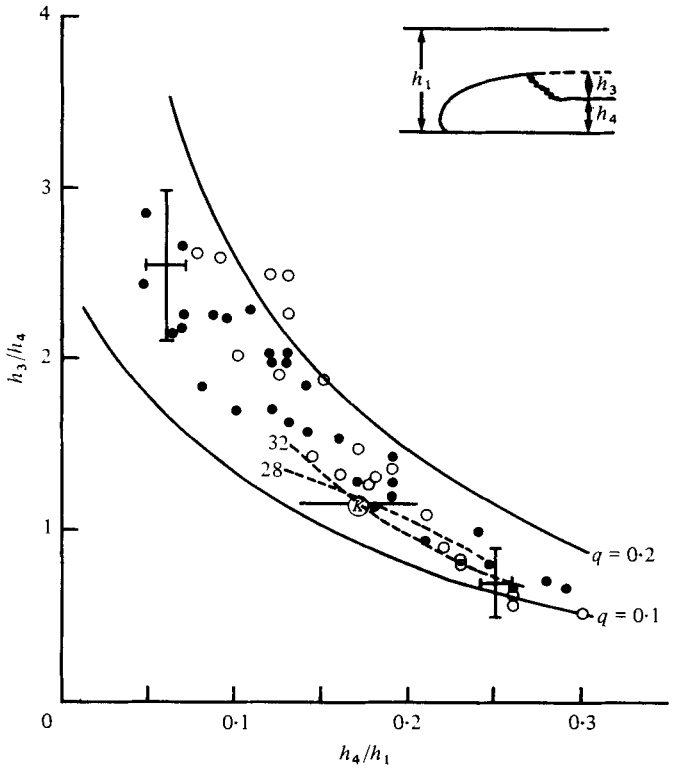

FIGURE 7. Values of the non-dimensional head-height h_3/h_4, plotted against the fractional depth of the flow. ○ from steady-state apparatus; ● from modified lock exchange. The theoretical curves for the volume flow $q = g'Q/U_1^3 = 0{\cdot}1$ and $0{\cdot}2$ are also plotted. The dashed lines are replotted from the work of Keulegan (1957). The line through the point K is at $h_3/h_4 = 1{\cdot}16$, the mean value quoted by Keulegan for all his experiments.

3.3. *Head height*

The mixing process at the gravity current head has a characteristic vertical extent h_3 and this results in a mixed zone behind the head and above the following gravity current of depth h_3 also. The measured depth of this region has been non-dimensionalized with h_4 and is plotted in figure 7 as a function of the fractional depth h_4/h_1. This non-dimensional head height decreases from over 3·0 at $h_4/h_1 \simeq 0{\cdot}05$ to about 0·6 at $h_4/h_1 \simeq 0{\cdot}3$. The open circles were obtained in the steady-state apparatus and the closed circles in the modified lock-exchange flow and there is no systematic difference between the flows outside the estimated experimental error shown by the perpendicular bars.

3.4. *Velocity and salinity profiles*

Profiles of mean velocity and mean salinity were made behind the gravity current head and a typical velocity profile is shown in figure 8. This profile is subject to error near zero velocity where poor linearization and small temperature changes make accurate velocity measurements difficult. Fortunately the velocity profile may be checked for its general form with dye-tracer experiments, a knowledge of the flux of dense fluid flowing into the gravity current head and the requirement of a no-slip

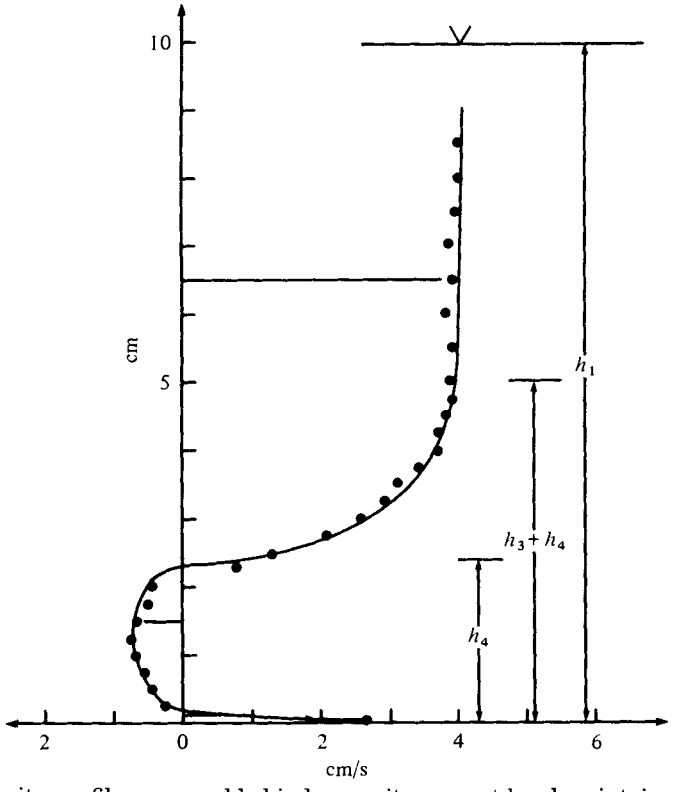

FIGURE 8. Velocity profile measured behind a gravity current head maintained in a steady state. Total depth $h_1 = 9{\cdot}8$ cm. The depth h_4 of the saline flow towards the gravity current head is 2·4 cm and the total head height (h_3+h_4) is 5·0 cm. $(\rho_2-\rho_1)/\rho_1 = 0{\cdot}004$ and $U_1 = 2{\cdot}7$ cm s^{-1}.

condition at the lower surface. The depths h_4 and (h_3+h_4) are taken from visual observations. The total depth, h_1, is 9·8 cm, the depth, h_4, of the saline flow (the gravity current) is 2·4 cm and the total head height (h_3+h_4) is 5·0 cm. The uniform mean velocity, U_1, approaching the gravity current head is 2·7 cm/s. The profile clearly shows a region above the head (of unmixed ambient fluid) with a nearly uniform velocity of 4·0 cm/s and below this is a mixed layer where the velocity decreases to near zero. The lowest layer is the gravity current proper of unmixed dense fluid in which the velocity profile indicates a maximum velocity of 0·8 cm/s of dense fluid approaching the stationary gravity current head. Close to the lower boundary is a reverse flow of dense fluid back along the moving wall at a maximum velocity equal to the wall velocity of 2·7 cm/s.

There is a net volume flux of dense fluid travelling towards the stationary gravity current head and to maintain a steady state this must equal the flux of dense fluid convected away from the gravity current head in the mixed region. If we revert to axes which have the lower wall stationary and the ambient fluid at rest, we see a gravity current head moving to the left at 2·7 cm/s, followed by a gravity current with a maximum velocity of $2{\cdot}7+0{\cdot}8 = 3{\cdot}5$ cm/s. Integration of this sketched velocity profile over the gravity current gives a total volume flux per unit width of dense fluid into the gravity current head of 1·17 cm^2/s of which 0·22 cm^2/s is carried forwards

only to be reversed back under the gravity current head near the lower boundary. This fluid occupies about the lower third of the gravity current. The volume flux per unit width of dense fluid into the gravity current head to be subsequently mixed with the less dense fluid is the difference $Q = 0{\cdot}95$ cm^2/s giving $Qg'/U_1^3 = 0{\cdot}19$ and $Q/U_1 h_4 = U_4/U_1 = 0{\cdot}15$. Thus the volume flux per unit width of dense fluid into the gravity current head is approximately $5Q/4$ of which $Q/4$ is reversed back under the gravity current head and Q is mixed with less dense fluid at the top of the gravity current head.

Several velocity profiles were best fitted to the form

$$1-\frac{U(h)}{U(h_3)} = \left(1-\frac{h}{h_3}\right)^m, \tag{1}$$

where $U(h)$ is the mean velocity in the mixing region a height h above the upper surface of the gravity current. This surface, the origin for the velocity and salinity profiles, was determined visually. Similarly the density profile which is constant at ρ_1 above the mixing region and constant at ρ_2 below the mixing region was fitted to a curve of the form

$$\frac{C(h)}{C(0)} = \left(1-\frac{h}{h_3}\right)^n, \tag{2}$$

where $C(h)$ is the concentration of the more dense fluid and $1-C(h)$ the concentration of the less dense fluid. We deduced $m = n = 4$ as the best fit to our data. The flux of the denser fluid mixed at the gravity current head and swept back behind the head may be estimated by integrating the product of velocity and concentration fields to give

$$Q = \frac{m}{(n+1)(m+n+1)} h_3 U(h_3). \tag{3}$$

From figure 5, $h_3 = 2{\cdot}6$ cm and $U(h_3) = 4{\cdot}0$ cm/s yields $Q = 0{\cdot}92$ cm/s, which compares favourably with the estimate of $Q = 0{\cdot}95$ cm^2/s from the integrated velocity profile in the gravity current.

3.5. *Height of foremost point*

A principal difference observed between a head advancing over a with-slip surface and one advancing over a no-slip surface is that in the latter the foremost point of the head is slightly elevated above the surface as shown by the indicators in figures 1, 3 and 4. This raising of the foremost point (and the lobe and cleft structure) has been observed in flows at very high Reynolds numbers, e.g. atmospheric sea-breeze fronts, haboobs (see Lawson 1971 and Turner 1973, figure 3.14). It was, in fact, the similarity in shape and apparent structure of the large-scale phenomena and the laboratory experiments that has stimulated the present study. The ratio of the height of the elevated foremost point to the total height of the gravity current is then a convenient shape parameter with which to consider the influence of scale (that is, Reynolds number). The Reynolds number was formed from the height of the head of the gravity current, h_3+h_4, and the velocity of advance of the gravity current head, U_1. This selection allows comparison with other existing data although a Reynolds number based on the depth of h_4 rather than h_3+h_4 is probably more fundamental. (They only differ by a factor of about 2.)

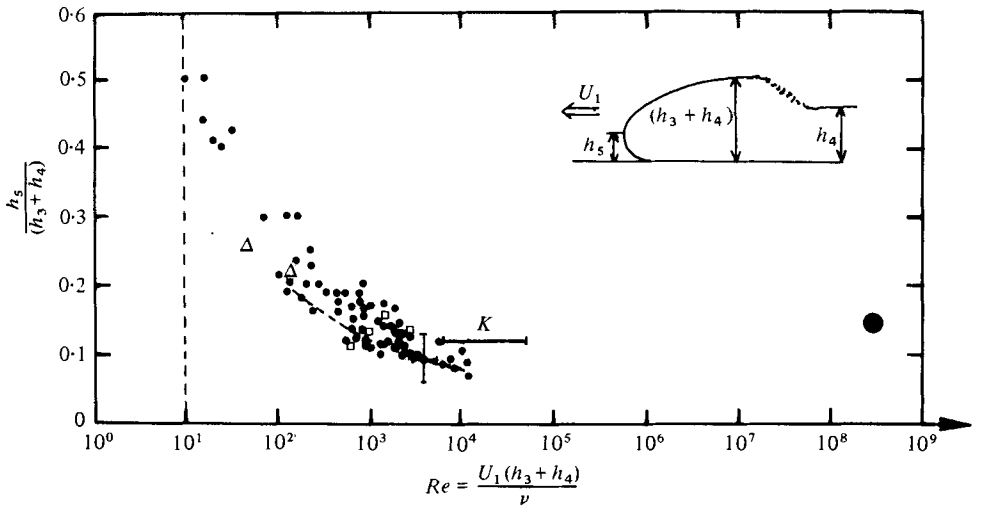

FIGURE 9. The variation of nose height, h_5, of a gravity current head with Reynolds number. h_5 is normalized with the total head height (h_5+h_4) and $Re = U_1(h_3+h_4)/\nu$. The dashed line is from Simpson (1972). △, □ and K are from the works of Braucher (1950), Wood (1965) and Keulegan (1958). ● is an atmospheric result from Lawson (1971).

The data plotted in figure 9 are taken from all our measurements (with no systematic differences between the results from the two techniques) together with data deduced from Braucher (1950), Keulegan (1958) and Wood (1965). The dashed curve is from the experiments of Simpson (1972). A single well-documented observation at very large Reynolds number is taken from Lawson (1971). The results have considerable scatter but clearly show a reduction in $h_5/(h_3+h_4)$ with increasing Reynolds number. No dependence of $h_5/(h_3+h_4)$ on the fractional depth was observed. For very small Reynolds number, less than approximately 10, a head is no longer distinct – an observation also recorded by Keulegan (1957). The ratio $h_5/(h_3+h_4)$ decreases from 0·5 to 0·15 between Reynolds numbers of 10 and 10^3, and above a Reynolds number of 10^3 the data might be interpreted as either a continuing decline, given by a continuation of the empirical curve of Simpson (1972), or as a near constant $h_5/(h_3+h_4)$. Keulegan (1958) gives only one measurement of $h_5/(h_3+h_4) = 0{\cdot}13$ without specifying the Reynolds number but states that the shape of the gravity current head is essentially independent of the Reynolds number in the range 7×10^3 to $5{\cdot}6 \times 10^4$. The single data point from Lawson (1971) at a very high Reynolds number also suggests that $h_5/(h_3+h_4)$ may be nearly independent of Reynolds number for $h_5/(h_3+h_4) \gtrsim 10^3$. Further discussion on this point is left until § 5.

4. A two-dimensional model of the flow

Our approach is to use the observations of § 3 to determine the more important features of the flow, neglect the influence of the rest and then develop a semi-empirical analysis requiring a minimum of empirical input.

Our observations, those of Simpson (1972), hypothetical flow fields sketched in Allen (1970, 1971) and recent experimental work of Winant & Bratkovich (1977) suggest that the ensemble-averaged flow field relative to a gravity current head is

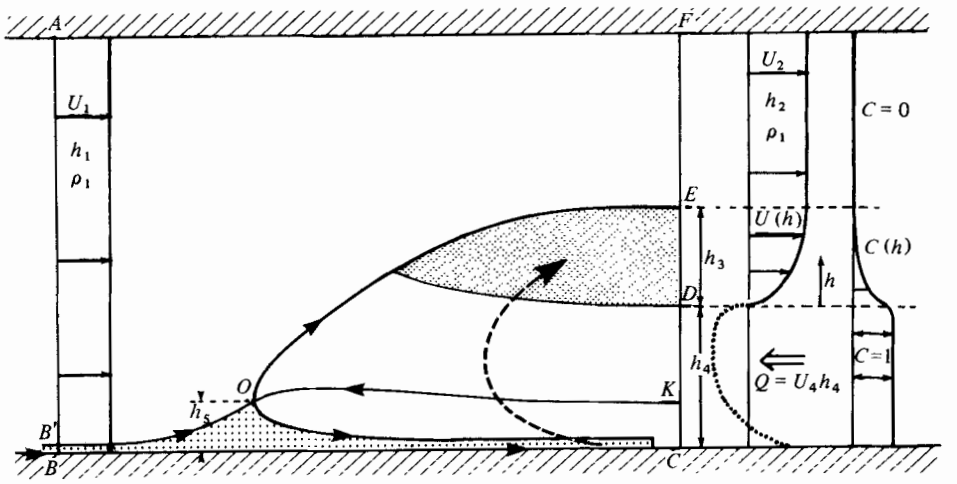

FIGURE 10. A two-dimensional model of the flow near a gravity current head in axes which hold the gravity current head stationary. At AB and FC the velocities are horizontal and the pressure hydrostatic. O is a stagnation point, $U(h)$, $C(h)$ are the profiles of velocity and concentration of the dense fluid in the flow close behind the head. U, h, ρ, refer to velocity, height and density, respectively.

that shown in figure 10 when the flow is between rigid surfaces. The less dense fluid approaches the gravity current head with uniform velocity U_1 and depth h_1 to bifurcate and flow either side of the head. The three streamlines separating the bifurcating fluid must meet a streamline from within the denser fluid at O. This last streamline divides the denser fluid that is reversed along the wall from the denser fluid that is mixed at the top of the gravity current. A small amount of the less dense fluid is ingested below the head eventually to arrive at the mixing region at the top of the head (indicated by the dashed arrow in figure 10). Nearly all the less dense fluid is accelerated over the head where some of it is mixed with the denser fluid. The surfaces AF and BC are moving to the right with velocities U_1. The velocity and salinity profiles are shown along a line $CKDEF$ behind the head where the velocities are horizontal and the pressure hydrostatic.

We now introduce some simplifying assumptions.

(*a*) The velocity above the head is a constant, U_2. Our measurements and those of BS showed this to be a good approximation over the observed range of h_4/h_1, that is $0{\cdot}33 \gtrsim h_4/h_1 \gtrsim 0{\cdot}05$. At smaller values of h_4/h_1, this approximation may be poor and we consider that flow later in this section.

(*b*) The depth $B'B$ is $O(10^{-1})$ of the height of the foremost point of the gravity current head and $O(10^{-2})$ of the total height of the head. The flux of less dense fluid flowing under the head is $O(10^{-1})$ of the dense fluid mixing at the top of the head. Thus the presence of the over-run less dense fluid may safely be neglected except for its role in allowing an elevated foremost point of the head.

(*c*) In our two-dimensional model the foremost point of the head is taken to be the stagnation point O, thus following models suggested by Benjamin (1968) and Allen (1971). We have no analytical justification for this but extensive experimental work using dye in both fluids does not contradict the supposition.

(*d*) Both the momentum change of the dense fluid reversed along the lower wall and the force applied at that wall as the result of shear stress there are small compared with relevant momentum changes and forces. This is supported by the conclusions of Abraham & Vreugdenhil (1971).

(*e*) The energy loss per unit volume along the streamline KO can be neglected compared with, say, $\rho g' h_4$.

To complete the analysis the following three numerical inputs from experiment will be required:

(i) The height, h_5, of the foremost point. We shall take the ratio $h_5/(h_3+h_4)$ as 0·125, independent of h_4/h_1 and typical of our measurements with $U_1(h_3+h_4)/\nu > 10^3$.

(ii) The shape parameters of the velocity and salinity profiles, using equations (1) and (2) in § 3.

(iii) The value of the mixing parameter $q = g'Q/U_1^3$, whose measured variation with fractional depth is shown in figure 6.

The analysis generally follows that of BS wherein the stagnation point O was on the surface. Bernoulli's equation is applied along the streamline $B'O$ and KO (the positions of B' and K are not required but the velocity at K is assumed uniform at Q/h_4), hydrostatic pressure is assumed everywhere that the flow is horizontal, a momentum balance is carried out on a control volume enclosing the head and the adjacent flow and the Boussinesq approximation is made. The resulting expression is

$$f - 2xf(1+\xi)^2 - 2\delta q f^2 \phi x(1+\xi)\beta^{-1} - 2q^2 f^3 \phi + q^2 f^3 + [1+\gamma\beta(1-\phi)(1+\beta\phi)^{-1}][2-\phi-\gamma B\phi(1-\phi)(1+B\phi)^{-1}] + B^2\phi x^{-2}(\gamma^2 - 2\epsilon) - 2h_5/h_4 = 0, \tag{4}$$

and application of the continuity equation yields

$$h_1/h_2 = (1+B\phi)(1-\phi)^{-1}, \quad h_3/h_4 = B(1-\phi)(1+B\phi)^{-1}, \tag{5), (6}$$

$$U_2/U_1 = (1+\xi)(1+B\phi)(1-\phi)^{-1}, \quad U_4/U_1 = qf, \tag{7), (8}$$

where

$$f = U_1^2/g'h_4, \quad \xi = (1-\alpha/\beta)qf\phi, \quad \phi = h_4/h_1,$$

$$B = qf\beta^{-1}(1+\xi)^{-1}, \quad x = (1+B\phi)(1-\phi)^{-1}, \quad q = Qg'/U_1^3$$

and

$$\alpha U_2 h_3 = \int_0^{h_3} U(h)\,dh, \quad \beta U_2 h_3 = \int_0^{h_3} C(h)\,U(h)\,dh,$$

$$\gamma h_3 = \int_0^{h} C(h)\,dh, \quad \delta U_2^2 h_3 = \int_0^{h_3} U^3(h)\,dh,$$

$$\epsilon h_3^2 = \int_0^{h_3} hC(h)\,dh.$$

Equation (4) is the same as that of BS except for the term $-2h_5/h_4$ on the left-hand side. This term is due to the elevation of the stagnation point O a distance h_5 above the surface. The equation (4) is a simple algebraic expression which gives the Froude number characterizing the rate of advance of the head, $f^{\frac{1}{2}} = U_1/(g'h_4)^{\frac{1}{2}}$, as a function of the depth ratio $\phi = h_4/h_1$ given the *form* of the velocity and salinity profiles in the mixed region and the variation of the position of the stagnation point h_5 and the non-dimensional mixing rate $q = Qg'/U_1^3$ as functions of h_4/h_1. Other length and velocity

ratios, equations (5)–(8), follow once the Froude number has been determined. To solve equation (4) the shape parameters α, β, γ, δ and ϵ were calculated using (1) and (2) and the ratio $h_5/(h_3+h_4)$ was taken as 0·125, independent of h_4/h_1.

Solutions for $U_1/(g'h_4)^{\frac{1}{2}}$ and h_3/h_4 are plotted in figures 5 and 7 for $q = 0{\cdot}1$ and 0·2, again typical of our experimental results. We note that the analysis is for flow between two rigid surfaces but application to a flow with a free upper surface is direct (see Benjamin 1968), the error in application being of the order of and generally less than the fractional density difference. To the accuracy of the Boussinesq approximation the analysis is applicable to the experimentally simpler configuration of a free surface at the upper boundary. Good agreement between the analysis and the experiments is observed, suggesting that the model not only contains the significant physical processes but also that they have been adequately modelled.

The interesting case of a head advancing into an effectively infinite depth of fluid is, unfortunately, difficult to obtain experimentally and it is uncertain whether $U_1/(g'h_4)^{\frac{1}{2}}$ (see figure 5) continues to increase as h_4/h_1 is reduced below the present minimum experimental value of $h_4/h_1 = 0{\cdot}05$. When the depth of the fluid into which the gravity current head is advancing is very large, equation (4) reduces to

$$-f+q^2f^2+2\left(1+\frac{\gamma}{\beta}qf-\frac{h_5}{h_4}\right)=0, \tag{9}$$

or in dimensional form

$$-U_1^2+U_4^2+2g'(h_4+\gamma h_3-h_5)=0. \tag{10}$$

The analysis on which this equation is based is, however, inapplicable in this limit as the assumption of uniform flow above the gravity current head must be poor. An alternative approach was used in Benjamin (1968) and BS in this limit. By taking A and F (see figure 10) to great heights, assuming hydrostatic pressure along AB and FC, using Bernoulli's equation (with no energy loss) from B' to O and K to O, requiring static pressure continuity at O and equal total head at A and F the same equations (9) and (10) are determined directly for the limit $h_4/h_1 \to 0$ without the assumption of uniform flow above the gravity current head. Assuming that the velocity and salinity profiles have the same form as $h_4/h_1 \to 0$, that $h_5/(h_3+h_4) = 0{\cdot}125$ as $h_4/h_1 \to 0$ and that $q = 0{\cdot}1$, say, as $h_4/h_1 \to 0$ (see figure 6), then (10) gives $U_1/(g'h_4)^{\frac{1}{2}} = f^{\frac{1}{2}} = 1{\cdot}50$ and $h_3/h_4 = qf/\beta = 2{\cdot}52$. Neither result is inconsistent with an extrapolation of the experimental data in figures 5 and 7 to $h_4/h_1 \to 0$.

5. Discussion

5.1. *General discussion*

The experimental apparatus described in § 2 made possible the study of gravity current heads in a steady state in isolation from the dynamics of the following gravity current and enabled several poorly understood aspects of the gravity current head to be observed in some detail. Intense mixing between the two fluids occurred at the head; the mixing resulting from a shear instability between the two fluids complicated by the gravitational instability of less dense fluid near the surface over-run by the head. The gravitational instability results in an unsteady three-dimensional flow (on the scale of the head) which has also been observed in atmospheric flows. The over-run fluid, the associated raising of the foremost point of the gravity current above the surface and the consequent gravitational instability and unsteady three-dimensional

flow are all absent when there is no stress at the surface below the head (see BS). In that flow the mixing between the two fluids was a result of a two-dimensional shear instability alone.

In both flows, with and without a surface stress, the gravity current fluid is mixed *out* of the gravity current at the head, the mixing fluid being left behind the gravity current head above the following gravity current, forming a thick velocity and density interface. To maintain a steady state this mixed fluid must be replaced from the following gravity current, requiring that the mean flow behind a gravity current head must be faster than the rate of advance of the head itself.

The experiments in the steady-state apparatus and some made with a modified lock-exchange flow enabled the collection of data over a wide range of the independent variable h_4/h_1, that is the ratio of the depth of the gravity current to the overall depths of the two fluids. Three dimensionless variables, which together characterize much of the flow near the head, namely $U_1/(g'h_4)^{\frac{1}{2}}$, Qg'/U_1^3 and h_3/h_4, were determined as functions of h_4/h_1. No significant difference was observed between results obtained with the steady-state apparatus and with the modified lock-exchange flow. The Froude number, $U_1/(g'h_4)^{\frac{1}{2}}$ and the ratio of mixed layer depth to gravity current depth, h_3/h_4, though functions of h_4/h_1, were both of order unity while the dimensionless mixing rate, Qg'/U_1^3, appeared to be a weaker function of h_4/h_1, of order 0·2. The ratio of the mean over-taking velocity in the gravity current to the velocity of advance of the gravity current, $U_4/U_1 = (Qg'/U_1^3)\,(U_1/(g'h_4)^{\frac{1}{2}})^{-2}$, is, thus, also of order 0·2.

Compared with the gravity current head running over a with-slip boundary, the dimensionless mixing ratio, Qg'/U_1^3, is larger, the Froude number, $U_1/(g'h_4)^{\frac{1}{2}}$, is smaller but the depth ratio, h_3/h_4, is similar when the boundary is without slip. The product $U_4/U_1 = (Qg'U_1)\,(U_1/(g'h_4)^{\frac{1}{2}})^{-2}$ is also similar in both experiments.

5.2. *The mixed layer depth*

A further aspect of the gravity current head is that although the shear instability between the two fluids is complicated by the gravitational instability of the over-run less dense fluid, a shear instability, billow growth and subsequent collapse to fine structure is still present. This has been observed and photographed (figure 6 of Simpson 1969), using slit lighting. The shadowgraph, figure 1, also gives an indication of instability, growth and collapse. The billow structure was quantified for one lock-exchange flow with $h_1 = 6$ cm, $h_4 = 1{\cdot}4$ cm, $U_1 = 2{\cdot}5$ cm s^{-1}, and $(\rho_2 - \rho_1)/\rho_1 = 0{\cdot}007$. Twenty-five billow growth patterns were measured. The billows grew to a mean maximum billow amplitude of $1{\cdot}4 \pm 0{\cdot}2$ cm. This was also the depth of the mixed layer, h_3. That is, although the coherent billow structure collapsed, a mean velocity and density profile remained over a depth equal to the maximum billow amplitude. This was also the case in BS when the shear instability was two-dimensional and more easily observed. The mean wavelength, λ, of the billows was $2{\cdot}4 \pm 0{\cdot}2$ cm and the ratio of these two lengths was $0{\cdot}6 \pm 0{\cdot}1$. This is smaller than but close to the ratio of $0{\cdot}8 \pm 0{\cdot}2$ observed in BS. Thorpe (1973), in a study of the Kelvin–Helmholtz instability between fluids of different density, found this ratio to be a function of an initial Richardson number, $g'l/(\Delta U)^2$, where l was a length characteristic of the interface thickness and ΔU the velocity difference across the interface. The ratio increases to about 0·5 as the initial Richardson number decreases to about 0·05. In the present experiments and those in BS the initial Richardson number is very small (essentially determined by

the Reynolds number, it was estimated to be less than 0·01 in both experiments), and the observed ratio of maximum billow amplitude to wavelength was to be expected for Kelvin Helmholtz instability with very small initial Richardson number. The very small initial Richardson number also results in the length scales characterizing the velocity and density profiles (effectively m and n) being equal (Thorpe 1973).

5.3. *Comparison with other work*

Probably the most thorough analytical treatment of gravity current heads is that of Benjamin (1968), which is an inviscid analysis based on the lock-exchange problem but also includes a solution for a gravity current running under a fluid of infinite depth. The analysis was for a cavity flow in which the fluids were immiscible but it was suggested that the results at $h_4/h_1 = 0$ could be extended to miscible fluids if h_4 was identified with the densimetric mean height of the fluid behind the gravity current head, that is taking into account the dense fluid mixed with the lighter fluid at the gravity current head and then left in the wakelike flow behind the head. Benjamin gave a solution for the Froude number $U_1/(g'h_4)^{\frac{1}{2}}$ as a function of the fractional depth h_4/h_1 with limits of $2^{-\frac{1}{2}}$ at $h_4/h_1 = \frac{1}{2}$ and $2^{\frac{1}{2}}$ at $h_4/h_1 = 0$. The present analysis reduces to Benjamin's when both $q = 0$ and $h_5/(h_3+h_4) = 0$ and a dashed curve corresponding to this solution has been included in figure 5 for comparison. The experimental results are less than the analytical result from Benjamin (1968) except at small h_4/h_1, where there is some measure of agreement. If h_4 was identified with the densimetric mean height of the fluid behind the gravity current the theoretical curve could be even higher, similar in fact to the experimental curve from BS (see figure 11), giving even less agreement.

In figure 11 we have plotted the variation of $U_1/(g'h_4)^{\frac{1}{2}}$ with h_4/h_1 determined from the present experiments together with that available in the literature. Abraham & Vreugdenhil (1971) give details of four lock-exchange experiments made at large values of h_4/h_1 (a_2/a_1 in their notation) from 0·27 to 0·35 with Reynolds numbers, U_1h_4/ν, between 14000 and 20000. Their data are plotted in figure 11 and they lie slightly above our results for the same fractional depth. Keulegan (1958), in a series of lock-exchange experiments, deduced that $U_1/(g'h_4)^{\frac{1}{2}} = 1{\cdot}05$ and that the gravity current head could be usefully described as a separate entity. No variation with h_4/h_1 was sought. We have extracted the values of $U_1/(g'h_4)^{\frac{1}{2}}$ during four experiments in which the values of h_4/h_1 are also recorded (table 1, Keulegan 1958), and have plotted smooth curves through the results in figure 11. (Note that Keulegan used a slightly different definition of g' but the difference will result in less than a 1% change in $U_1/(g'h_4)^{\frac{1}{2}}$).

Several other authors have examined the advance of gravity current heads in lock-exchange flows but have given a velocity of advance non-dimensionalized with g' and the total depth of the two fluids, e.g. Yih (1965), Barr (1967), or with the total head height (Middleton 1966).

Although the total head height (h_3+h_4) is the most obvious characteristic length of the gravity current head both in the laboratory and at larger scales, the ratio of (h_3+h_4) to the depth of the following gravity current is not often reported. Keulegan (1958) gave a mean value of this ratio to be 2·16 from many experiments at unspecified fractional depths h_4/h_1 (the mean value of h_4/h_1, for all his experiments, was about 0·17). The mean of Keulegan's data, that is $(h_3+h_4)/h_1 = 2{\cdot}16$, for $h_4/h_1 = 0{\cdot}17$ is in

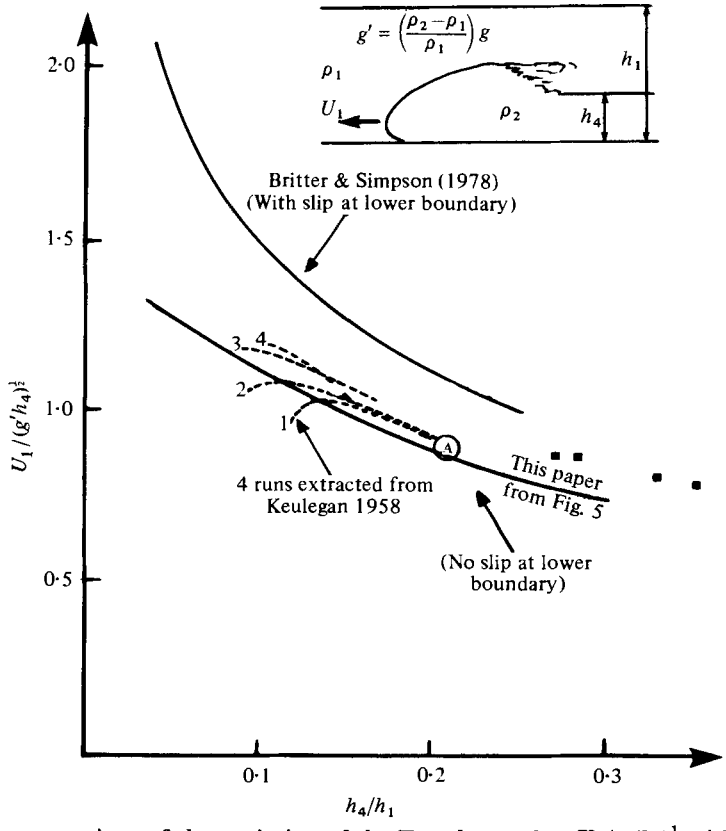

FIGURE 11. A comparison of the variation of the Froude number $U_1/(g'h_4)^{\frac{1}{2}}$ with the fractional depth h_4/h_1 with the experimental results of other authors. The lower solid curve is the mean of the data in figure 5. The dashed lines 1, 2, 3, 4 have been constructed from Table 1, Keulegan (1958). The data ■ are from Abraham & Vreugdenhil (1971) and Ⓐ is from a documented sea-breeze front (see § 5). The upper solid curve is from BS and is for a gravity current running over a surface with slip.

accord with the data plotted in figure 7. If we replot some of Keulegan's results to show the variation of h_3/h_4 with the fractional depth, h_4/h_1, instead of travel distance, a clear variation of h_3/h_4 with h_4/h_1 is obtained for a great part of each experiment. In figure 7 traces from Keulegan's (1957) figures 28 and 32 show close agreement with the present results.

5.4. *Influence of Reynolds number*

Many of the problems to which the results of this paper might be directed (see § 1) are at Reynolds numbers (however defined) of 10^5 to 10^9, outside the range of the present laboratory experiments and outside the range of laboratory experiments in general. It is, therefore, essential to consider in what ways the flow at larger Reynolds numbers might be different from the laboratory experiments. Keulegan (1957) and Barr (1967) found that the dimensionless velocity of advance was strongly Reynolds number dependent for $Re \gtrsim O(10^3)$ and suggested Reynolds number independence for $Re \lesssim O(10^3)$. Keulegan, however, noted that there was still a slight increase in $U_1/(g'h_4)^{\frac{1}{2}}$ with Reynolds number even for $Re \lesssim O(10^3)$. A comparison of the present

data with that from Keulegan (1957) and Abraham & Vreugdenhil (1971) also indicate that $U_1/(g'h_4)^{\frac{1}{2}}$ increases slightly with Reynolds numbers when $Re \gtrsim O(10^3)$. The shape parameters plotted in figure 9, the ratio of the foremost part of the head, h_5, to the overall height of the head, h_3+h_4, also shows a strong Reynolds number dependence for $Re \lesssim O(10^3)$. Above $Re \sim O(10^3)$ the data is neither extensive nor accurate enough to distinguish between a continuing decline in $h_5/(h_3+h_4)$, approximately proportional to $Re^{-\frac{1}{4}}$, or as nearly constant. Reference to the analysis in §4 indicates that a decreasing $h_5/(h_3+h_4)$ with increasing Re would give $U_1/(g'h_4)^{\frac{1}{2}}$ increasing slightly with Re. However if $h_5/(h_3+h_4) \to 0$ as $Re \to \infty$ then, quite apart from the correctness of the model in §4 the flow will be similar to the inviscid flow studied in BS with $U_1/(g'h_4)^{\frac{1}{2}}$ as given in figure 11. The assumptions and approximations introduced in §4 must become valid in the limit $Re \to \infty$ if $h_5/h_3+h_4) \to 0$ also. However the data from Lawson (1971) has $h_5/(h_3+h_4) \sim O(10^{-1})$ at $Re \sim O(10^8)$, that is $h_5/(h_3+h_4)$ is the same at $Re \sim O(10^3)$ and $Re \sim O(10^8)$. Other data also indicate that $h_5/(h_3+h_4)$ is significantly different from zero at very large Reynolds numbers, e.g. see the frontispiece to Yih (1965) and figure 3.14 of Turner (1973), where the consequent lobe and cleft structure is present.

We have compared our experimental results with a large-scale, high Reynolds number gravity current head – a sea breeze front. A well-documented sea breeze front was described by Simpson *et al.* (1977) as a flow 300 m deep of air 1·4 °C colder than its surroundings advancing at 3·5 m s^{-1} beneath a sharp inversion at 1400 m. The inversion was found to be only slightly displaced by the sea breeze flow and its height will be taken to correspond to h_1. Thus with $h_1 = 1400$ m, $g' = 0{\cdot}047$ m s^{-3} and $h_4 = 300$ m the Froude number $U_1/(g'h_4)^{\frac{1}{2}}$ is 0·93 at a fractional depth of 0·21. These measurements at a Reynolds number of approximately 10^8 are consistent with the experimental results of this paper. The maximum velocity in the flow behind the sea breeze front was 5 m s^{-1} and if we *assume* a velocity profile similar to that in figure 8 then $U_4/U_1 = 0{\cdot}29$ and $q = Qg'/U_1^3 = 0{\cdot}35$. Both results are larger than but still comparable to the laboratory results. The ratio of the maximum depth of a sea breeze flow at the front to the following steady flow was obtained on this and two other occasions. This ratio was close to 2 so the head height ratio h_3/h_4, is approximately 1, which is also consistent with the laboratory results for $h_4/h_1 = 0{\cdot}21$ (figure 7). Thus, taken overall, there is a good degree of consistency between the laboratory experiments and the full scale flow.

We thank Mr M. Cantwell and Mr R. Flatt for their work on the apparatus, which was originally constructed at the University of Reading and later transferred to Cambridge. J.E.S. is supported by a grant from the Natural Environment Research Council and R.E.B. is supported by a grant from Shell Research Ltd, Thornton.

REFERENCES

ABRAHAM, G. & VREUGDENHIL, C. B. 1971 Discontinuities in stratified flow. *J. Hydraul. Res.* **9**, 292–308.

ALLEN, J. R. L. 1970 *Physical Processes of Sedimentation*, p. 191. London: George Allen and Unwin.

ALLEN, J. R. L. 1971 Mixing at turbidity current heads, and its geological implications. *J. Sedimentary Petrology* **41**, 97–113.

BARR, D. I. H. 1967 Densimetric exchange flow in rectangular channels. III. Large scale experiments. *Houille Blanche* **22**, 619–631.

BENJAMIN, T. B. 1968 Gravity currents and related phenomena. *J. Fluid Mech.* **31**, 209–248.

BRAUCHER, E. 1950 Initial characteristics of density current flow. M.I.T. Thesis.

BRITTER, R. E. & SIMPSON, J. E. 1978 Experiments on the dynamics of a gravity current head. *J. Fluid Mech.* **88**, 223–240.

HALL, F. F., NEFF, W. D. & FRAZIER, T. V. 1976 Wind shear observations in thunderstorm density currents. *Nature* **264**, 408–411.

HOULT, D. P. 1972 Oil spreading on the sea. *Ann. Rev. Fluid Mech.* **4**, 341–368.

KÁRMÁN, T. VON 1940 The engineer grapples with non-linear problems. *Bull. Amer. Math. Soc.* **46**, 615–683.

KEULEGAN, G. H. 1957 An experimental study of the motion of saline water from locks into fresh water channels. *U.S. Nat. Bur. Stand. Rep.* no. 5168.

KEULEGAN, G. H. 1958 The motion of saline fronts in still water. *U.S. Nat. Bur. Stand., Rep.* no. 5831.

LAWSON, T. J. 1971 Haboob structure at Khartoum. *Weather* **26**, 105–112.

MIDDLETON, G. V. 1966 Experiments on density and turbidity currents. I. Motion of the head. *Canadian J. Earth Sciences* **3**, 523–546.

O'BRIEN, M. P. & CHERNO, J. 1934 Model law for motion of salt water through fresh. *Trans. Amer. Soc. Civ. Eng.* **99**, 576–594.

SIMPSON, J. E. 1969 A comparison between laboratory and atmospheric density currents. *Quart. J. Roy. Met. Soc.* **95**, 758–765.

SIMPSON, J. E. 1972 Effects of the lower boundary on the head of a gravity current. *J. Fluid Mech.* **53**, 759–768.

SIMPSON, J. E., MANSFIELD, D. A. & MILFORD, J. R. 1977 Inland penetration of sea-breeze fronts. *Quart. J. Roy. Met. Soc.* **103**, 47–76.

THORPE, S. A. 1973 Experiments on instability and turbulence in a stratified shear flow. *J. Fluid Mech.* **61**, 731–751.

TURNER, J. S. 1973 *Buoyancy Effects in Fluids.* Cambridge University Press.

WINANT, C. D. & BRATKOVICH, A. 1977 Structure and mixing within the frontal region of a density current. *Proc. 6th Austr. Hydraulics & Fluid Mech. Conf., Adelaide, Australia*, pp. 9–11.

WOOD, I. R. 1965 Studies in unsteady self preserving turbulent flows. *Univ. N.S.W., Manly Vale, N.S.W. Australia. Rep.* no. 81.

YIH, C.-S. 1965 *Dynamics of Non-homogeneous Fluids.* Macmillan.

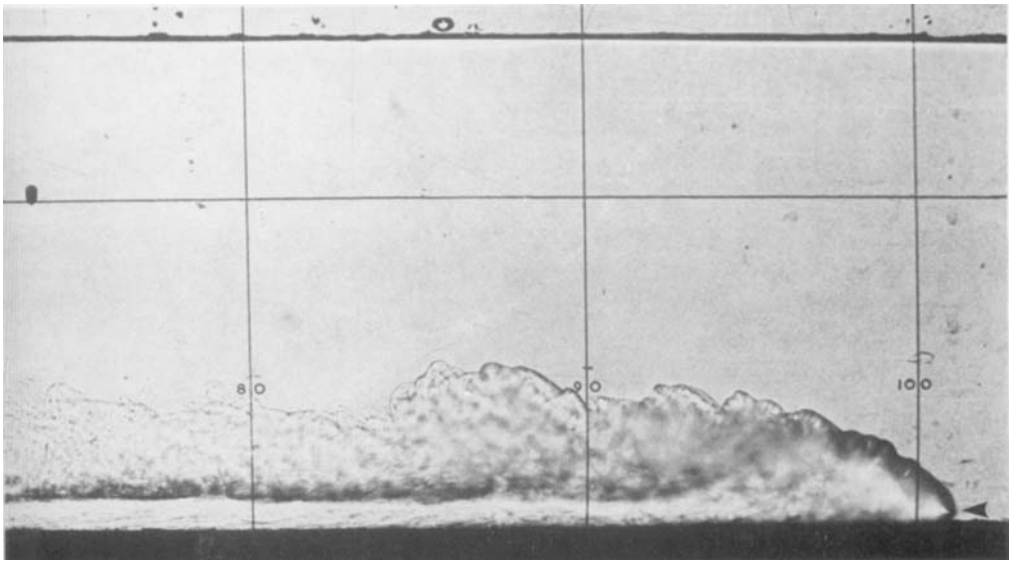

FIGURE 1. Shadowgraph of a gravity current head, passing the 100 cm mark from a lock extending from 0 to 20 cm, filled to a quarter of its depth with dense fluid. h_4/h_1 is 0·06 and the total head height is 4·5 times the depth of the following flow. $(\rho_2-\rho_1)/\rho_1 = 0{\cdot}008$. The arrow indicates the elevated foremost point.

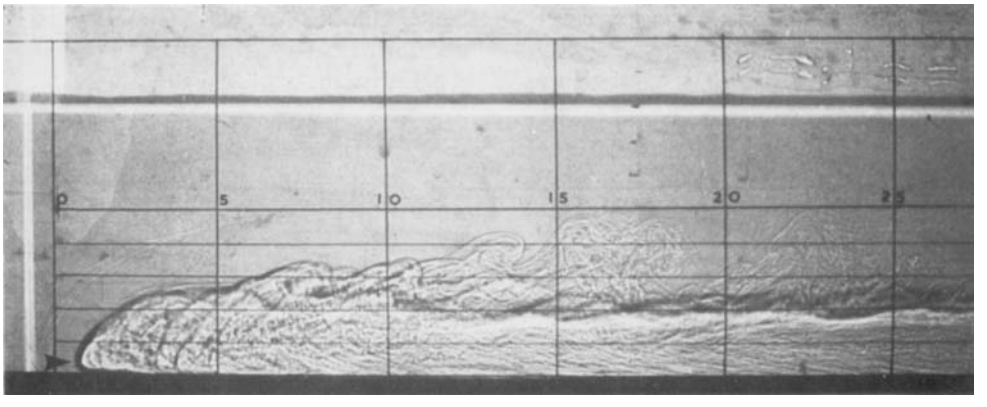

FIGURE 3. Shadowgraph of a gravity current brought to rest in a steady state. $(\rho_2-\rho_1)/\rho_1 = 0{\cdot}0074$; $h_1 = 8$ cm. The arrow indicates the elevated foremost point.

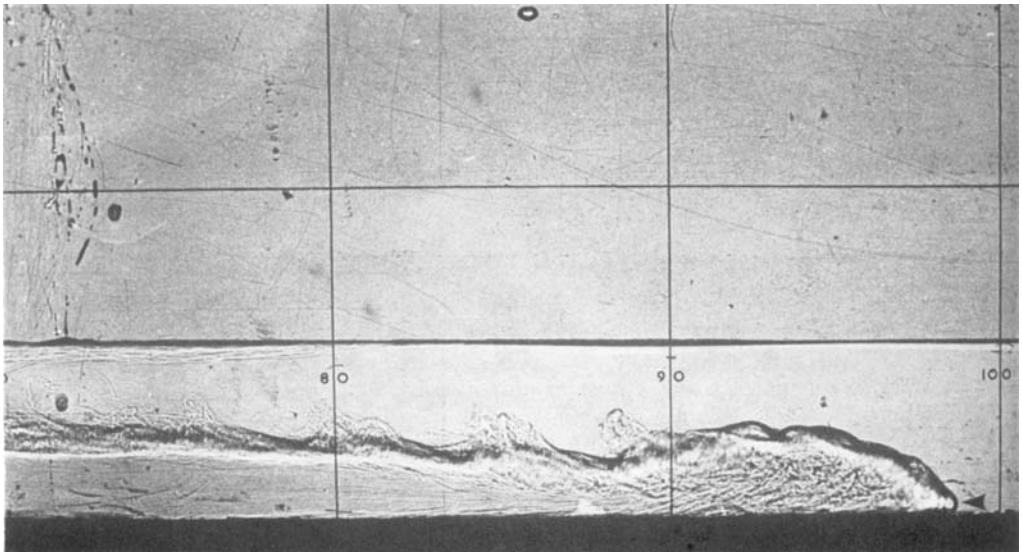

FIGURE 4. Shadowgraphs of gravity current head in lock-exchange flow. Central gate previously at left-hand edge of photograph. $h_1 = 5$ cm, $(\rho_2 - \rho_1)/\rho_1 = 0{\cdot}0074$; $h_4/h_1 = 0{\cdot}33$. Units are marked in cm. The arrow indicates the elevated foremost point.